HYDROTHERMAL SYNTHESIS
OF METAL-ORGANIC FRAMEWORK MIL–101

Vo Thi Thanh Chau[1], Hoang Van Duc[2]*

[1] Faculty of Technology, Quang Ngai Campus, Industrial University of Ho Chi Minh City,
12 Nguyen Van Bao St., Go Vap District, Ho Chi Minh City, Vietnam
[2] HU – University of Education, 34 Le Loi St., Hue, Vietnam

Abstract: In the present paper, a synthesis of MIL–101 with the hydrothermal process is demonstrated. The obtained material was characterized using powder X-ray diffraction (PXRD), transmission electron microscope (TEM), nitrogen adsorption/desorption isotherms at 77 K. The results showed that MIL–101 synthesized under optimal conditions exhibited high crystallinity and large surface area. The obtained MIL–101 possesses high stability in water and several organic solvents at their boiling point.

Keywords: MIL–101, hydrothermal synthesis, metal-organic framework

1   Introduction

Metal-organic frameworks (MOFs) are organic-inorganic hybrid materials with three-dimensional frameworks *via* strong metal-ligand bonds between metal cations and organic linkers [1, 2]. Since their discovery, MOFs have received a remarkable attention owing to their potential applications in gas storage [3, 4, 5], separation [6], and heterogeneous catalysis [7, 8]. MIL–101, which is one of the most popular MOFs, was first reported by Férey et al. in 2005 [9]. They showed that MIL–101 can be synthesized from $HF–Cr(NO_3)_3$, 1,4 dicarboxylic acid (H_2BDC), and H_2O. Since the discovery of large-pore MIL–101, several researchers have tried to manufacture MIL–101 for gas adsorption. However, it was difficult to obtain MIL–101 with a large BET surface of more than 3200 m^2/g [7] because of the presence of H_2BDC or inorganic impurities inside or outside pores. It is obvious that the synthesis of MIL–101 requires complicated techniques to completely remove non-reacted H_2BDC present both outside and within the pores of MIL–101. Yang et al. [3] used various alkalis such as potassium hydroxide (KOH), tetramethyl ammonium hydroxide (TMAOH), triethylamine ($(C_2H_5)_3N$), dimethylamine (C_2H_7N), methylamine (CH_5N), and ammonia (NH_3) to enhance the crystallization of MIL–101 and avoid recrystallization of H_2BDC. The $TMAOH–Cr(NO_3)_3–H_2BDC–H_2O$ system was suitable for obtaining MIL–101 with good surface properties. Hong et al. [7] reported a separation process in which a huge amount of H_2BDC was separated with a fritted glass filter, and then excess dissolution with hot solvents, such as ethanol, N,N-dimethyl-formamide, and NH_4F. The aim of this study is to find the optimal conditions for the synthesis of MIL–101 using the $H_2BDC–Cr(NO_3)_3–H_2O$ system.

---

* Corresponding: hoangvanduc2013@gmail.com

In the present paper, the effect of the synthesis conditions on the formation of MIL–101 as well as its hydrothermal stability in various solvents and conditions is demonstrated.

2   Experimental

Chromium (III) nitrate nonahydrate ($Cr(NO_3)_3 \cdot 9H_2O$), benzene 1,4-dicarboxylic acid ($C_6H_4(COOH)_2$, and hydrogen fluoride (HF, 40%) were purchased from Merck.

MIL–101 was synthesized according to a modified method [9]. The mixture containing H_2BDC, $Cr(NO_3)_3$, HF, and H_2O was heated in a teflon-lined stainless steel autoclave at 200 ºC for 8 hours. The resulting green solid materials were filtered and then extracted with ethanol in a soxhlet apparatus for approximately 12 hours to remove the amount of H_2BDC still present in the product. In the present work, the effect of the molar ratio of chromium nitrate to H_2BDC (Cr/H_2BDC) and water to H_2BDC (H_2O/H_2BDC) on the formation of MIL–101 is studied.

For the former, a mixture of 10^{-2} mol of H_2BDC, x mol of $Cr(NO_3)_3 \cdot 9H_2O$, 0.25×10^{-2} mol of HF and 265×10^{-2} mol of H_2O, with x taking the following values of 0.5×10^{-2}, 0.75×10^{-2}, 1.00×10^{-2}, 1.25×10^{-2}, 1.50×10^{-2}, and 1.75×10^{-2}. The samples are denoted as M–0.5, M–0.75, M–1.00, M–1.25, M–1.50, and M–1.75.

For the latter, a mixture of 10^{-2} mol of H_2BDC, 1.25×10^{-2} mol of $Cr(NO_3)_3 \cdot 9H_2O$, 0.25×10^{-2} mol of HF and y mol of H_2O, with y taking the values of 200×10^{-2}, 265×10^{-2}, 350×10^{-2}, 400×10^{-2}, 500×10^{-2}, and 700×10^{-2}. The samples are denoted as M200, M265, M350, M400, M500, and M700.

In both experiments, the water volume was kept constant at 100 mL.

Powder X-ray diffraction (XRD) was carried out on a D8–Advance (Brucker, Germany) with Cu Kα (λ = 1.5406 Å) radiation. Transmission electron microscopy (TEM) observations were obtained on a JEOL JEM–2100F. Nitrogen adsorption/desorption isotherm measurements were conducted using a Micromeritics 2020 volumetric adsorption analyzer system. Samples were pretreated by heating under vacuum at 150 °C for 3 hours.

3   Results and discussion

3.1   Synthesis of MIL–101 and its stability in various conditions

The PXRD patterns for MIL–101 material synthesized with different molar ratios of Cr/H_2BDC are shown in Figure 1a. At a low ratio of chromium to H_2BDC, the XRD pattern of M–0.50, M–0.75 and M–1.00 is similar to those reported by others [3, 4, 7], in which the main diffractions of MIL–101 in the 2θ range of 2.5–10° are observed. At a higher ratio of chromium to H_2BDC, a sharp and strong diffraction at 2θ around 1.7° appears as in the simulated pattern of MIL–101 [9] indicating the strong effect of the Cr/H_2BDC ratio on the formation of the MIL–101 structure.
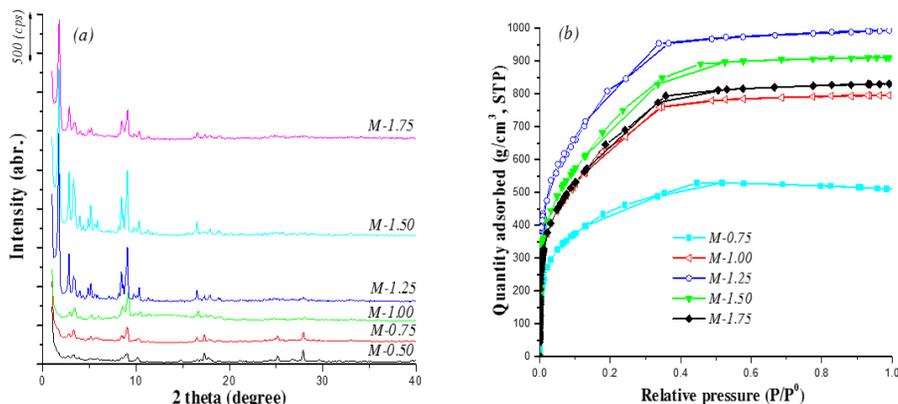
Fig. 1. (a) PXRD patterns and (b) isotherms of nitrogen adsorption/desorption of MIL–101 synthesized with different molar ratios of Cr/H_2BDC

The TEM images of MIL–101 materials synthesized with different molar ratios of Cr/H_2BDC are shown in Figure 2. It can be seen that the crystals are of an octahedron shape with varied sizes, depending on the molar ratios of Cr/H_2BDC, in the range of 230–570 nm. The size of particles reaches a minimum at sample M–1.25 (Table 1).

The textural properties of MIL–101 samples synthesized at different ratios of Cr/H_2BDC were investigated using the N_2 adsorption-desorption isotherm at 77 K as shown in Figure 1b. The isothermal curves are of type IV, with pore-filling steps at $p/p^0 \approx 0.2$ and $p/p^0 \approx 0.3$. This reveals the presence of two types of narrow mesopores [7]. The parameters characterizing the textural properties of the obtained MIL–101 materials are displayed in Table 1. The specific surface area and pore volume tend to increase with the increase of the Cr/H_2BDC molar ratio from 0.75 to 1.25, then decrease with the increase of the H_2O/CTAB molar ratio from 1.25 to 1.75. Hence, the suitable ratio of Cr/H_2BDC for the synthesis of MIL–101 was 1.25.
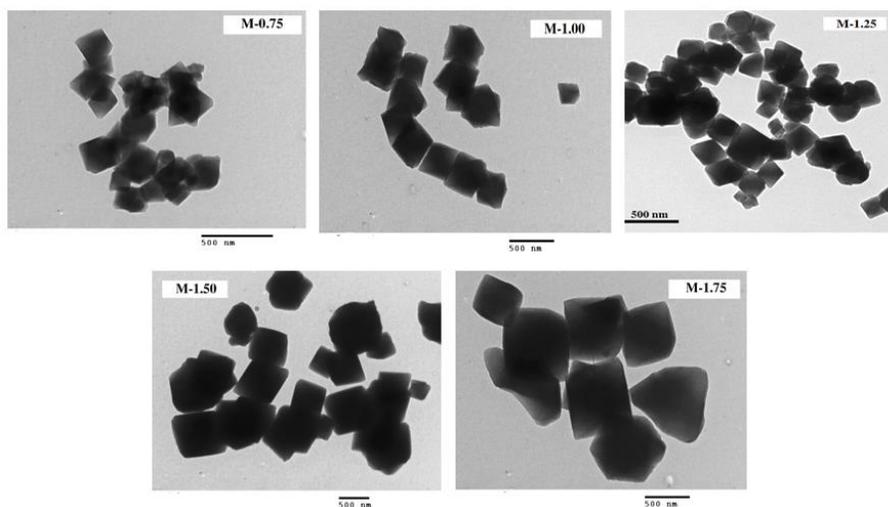

Fig. 2. TEM images of MIL–101 synthesized with different molar ratios of Cr/H_2BDC

Table 1. Textural properties of MIL–101 samples synthesized with different molar ratios of Cr/H₂BDC

Samples	S_{BET} (m².g⁻¹)	V_{pore} (cm³.g⁻¹)	$d*_{TEM}$ (nm)
M–0.75	1582	0.79	231
M–1.00	2328	1.23	376
M–1.25	2946	1.53	216
M–1.50	2642	1.41	522
M–1.75	2414	1.28	573

*Mean value counted from 100 particles

Figure 3a demonstrates the PXRD results of MIL–101 material synthesized with different molar ratios of H₂O/H₂BDC. The results show a considerable effect of the water amount in the composition of the reactants on the formation of the MIL–101 structure. All the samples with the increase in the molar ratios of H₂O/H₂BDC from 200 to 700 have the characteristic diffraction of MIL–101. Nevertheless, the peak at around $2\theta \approx 1.7°$ characterizing the mesoporous structure does not appear in the samples with high water content (M–500, M–700), while it is clearly observed in samples having lower water content (M–200 to M–400). In addition, when there is a higher water content in the reactant mixtures, a lower peak intensity is observed, indicating that water in the reactant mixtures plays an important role in the formation of the materials in terms of both morphology and crystallinity.
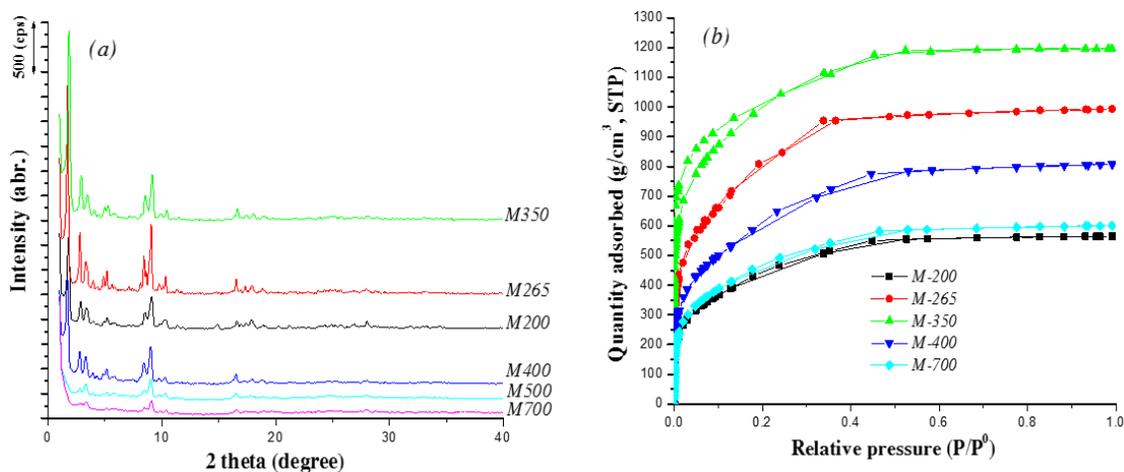

Fig. 3. (a) PXRD patterns and (b) isotherms of nitrogen adsorption/desorption of MIL–101 synthesized with different molar ratios of H₂O/H₂BDC

The water amount in the reactant mixtures also has a significant effect on the particle size of MIL–101 (Figure 4). In fact, the mean size of the material synthesized with a low water amount is 298 nm, 243 nm, and 364 nm for M200, M265, and M350, respectively. Meanwhile, when the amount of water increases further, the mean size decreases tremendously to 111 nm for M400, 173 nm for M500 and 137 nm for M700. It can be explained that high water content probably leads to a greater reduction of the crystal growth rates [10]. Furthermore, the H₂BDC

crystals are seen clearly in the M700 sample. This indicates that the perfect MIL–101 crystal cannot be achieved at a very high water content in the reactant mixture. It is clear that the biggest MIL–101 crystal is achieved in the M350 sample.
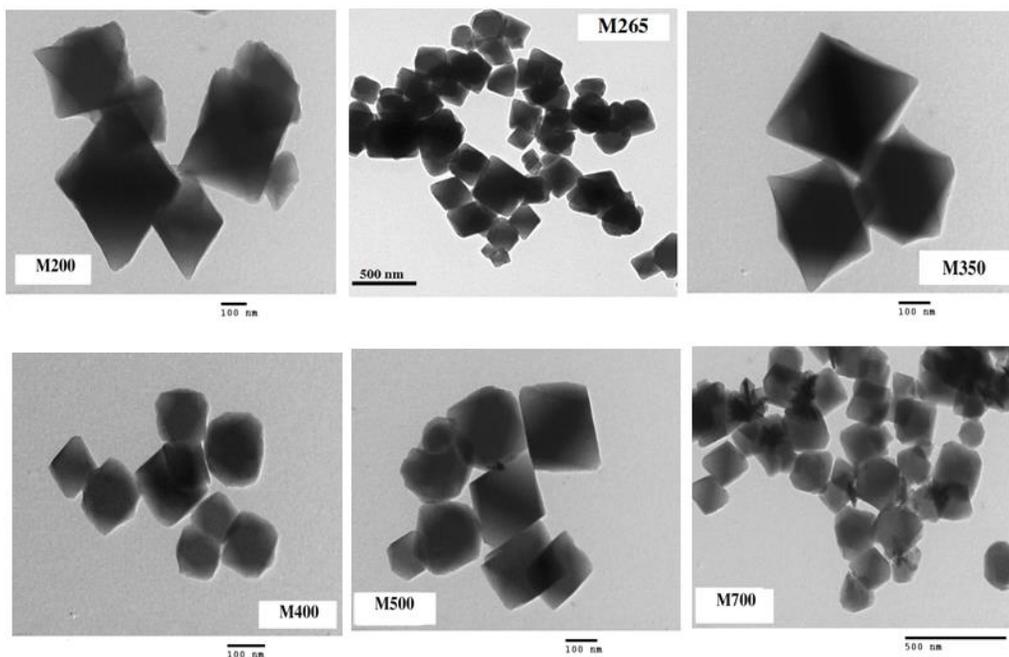

Fig. 4. TEM images of MIL–101 synthesized with different molar ratios of H_2O/H_2BDC

The nitrogen adsorption/desorption isotherms and texture properties of MIL–101 synthesized with different H_2O/H_2BDC molar ratios are illustrated in Figure 3b and Table 2. The results in Figure 3b show that the isotherms of the obtained samples correspond to the typical type IV with the presence of the hysteresis loop at a relative pressure of 0.2 and 0.4. The data in Table 2 indicate that the specific surface and pore volume increase when the H_2O/H_2BDC molar ratio increases from 200 to 350, and decrease when this ratio increases from 350 to 700. The M350 sample has the highest surface area and pore volume of 3586 $m^2.g^{-1}$ and 1.85 $cm^3.g^{-1}$, respectively.

Table 2. Textural properties of MIL–101 samples synthesized with different molar ratios of H_2O/H_2BDC

Samples	S_{BET} ($m^2.g^{-1}$)	V_{pore} ($cm^3.g^{-1}$)	d^*_{TEM} (nm)
M200	1618	0.87	298
M265	2946	1.53	216
M350	3586	1.85	364
M400	2274	1.25	111
M700	1708	0.93	137

The mean value counted from 100 particles

Figures 5a and 5b show the stability of MIL–101 with time under air conditions. MIL–101, as synthesized, was used as a control to compare the surveyed samples. Generally, the main characteristic peaks of MIL–101 are present in all PXRD patterns. However, the peak at around $2\theta \approx 1.7°$ is not present in samples exposed to ambient conditions for 15 days to 30 days without drying before the XRD measurements were carried out (Figure 5a). It is worth noting that this peak is clearly seen in the same sample if it is dry although it was exposed to humid air up to a year (Figure 5b). The disappearance of the characteristic peak of the mesoporous structure at small angles indicates that the material structure seems to be unstable in humid air. This is why this diffraction peak at 1.7° is reported in some papers [9] but not in others [3, 5, 7]. The stability of this peak is not well understood, but it has been thought that water in humid air blocks parts of the pore holes resulting in the change of the material structure and thus the disappearance of the characteristic diffraction of the mesoporous structure at around 1.7°. Therefore, this peak is only observed after the samples are dried.
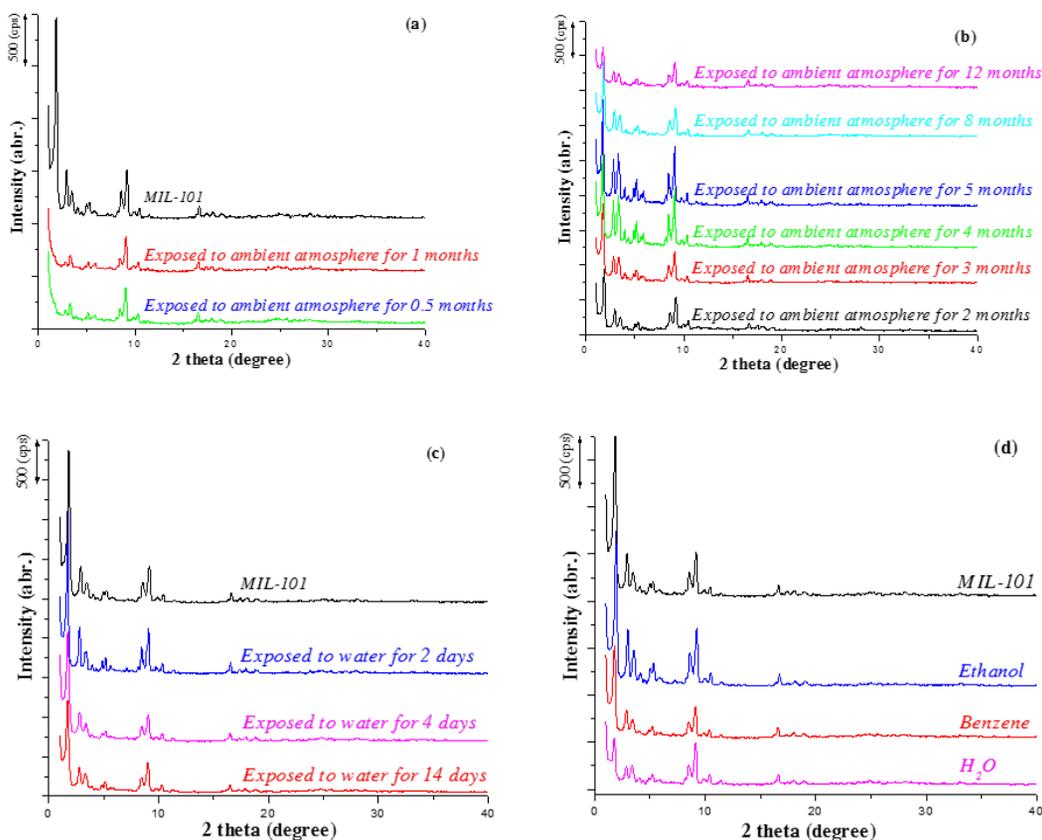

Fig. 5. PXRD patterns of MIL–101 exposed to ambient atmosphere for several months with (a) MIL–101 sample tested without drying; (b) MIL–101 samples dried at 100 °C for 12 h before testing; (c) MIL–101 exposed to water for several days; (d) MIL–101 exposed to several solvents at boiling temperature

The PXRD patterns of MIL–101 material in water at room temperature are presented in Figure 5c. It is clearly seen that the characteristic diffractions of MIL–101 remain in all PXRD patterns. Notably, the presence of the characteristic diffraction of the mesoporous structure at

around 1.7° reveals that the material remains stable after it has been soaked in water for several days.

The MIL–101 material was also soaked in water, benzene, and ethanol at their boiling temperature for 8 hours to study the stability. The results of PXRD (Figure 5d) indicate that MIL–101 also remains stable under these conditions, which is in good agreement with what reported by Hong et al. [7]. Moreover, all the characteristic diffractions of MIL–101 still remain at high intensity, suggesting that its structure does not collapse. Meanwhile, other highly cited MOFs such as MOF–177 and MOF–5 have relatively high thermal and chemical stability, and they are known to change and easily decompose in the presence of moisture [11, 12]. The fact that MIL–101 is rather stable in both polar and non-polar solvents at high temperature makes it an attractive candidate for various practical applications.

4   Conclusion

The molar ratio Cr/H_2BDC and H_2O/H_2BDC of 1.25 and 350, respectively, has significant effects on the textural properties as well as particle size. They provide the MIL–101 material with a large surface area and high crystallinity. The presence of a large amount of water in the reaction gel significantly reduces the particle size and crystallinity of the synthesized material. MIL–101 can be exposed to ambient air for several months without changing its crystalline properties, and it is also stable in water, benzene, and ethanol at their boiling point for several hours.

References

1. Janiak C., Vieth J. K. (2010), MOFs, MILs and more: concepts, properties, and applications for porous coordination networks (PCNs), *New J. Chem.*, 34(11), pp. 2366–2388.

2. Yaghi O. M., Keeffe M. O., Ockwig N. W., Chae H. K. (2003), Reticular synthesis and the design of new materials, *Nature*, 423, pp. 705–714.

3. Yang J., Zhao Q., Li J., Dong J. (2010), Synthesis of metal–organic framework MIL–101 in TMAOH–Cr(NO_3)$_3$–H_2BDC–H_2O and its hydrogen-storage behavior, *Microporous and Mesoporous Mater.*, 130, pp. 174–179.

4. Yang K., Sun Q., Xue F., Lin D. (2011), Adsorption of volatile organic compounds by metal–organic frameworks MIL–101: Influence of molecular size and shape, *J. Hazard. Mater.*, 195, pp. 124– 131.

5. Zhang Z., Huang S., Xian S., Xi H., Li Z. (2011), Adsorption equilibrium and kinetics of CO_2 on chromium terephthalate MIL–101, *Energy Fuels*, 25, pp. 835–842.

6. Ma S., Sun D., Wang X. S., Zhou H. C. (2007), A mesh-adjustable molecular sieve for general use in gas separation, *Angew. Chem., Int. Ed.*, 46(14), pp. 2333–2543.

7. Hong D. Y., Hwang Y. K., Serre C., Férey G., Chang J. S. (2009), Porous chromium terephthalate MIL–101 with coordinatively unsaturated sites: Surface functionalization, encapsulation, sorption and catalysis, *Adv. Funct. Mater.*, 19, pp. 1537–1552.

8. Saedi Z., Tangestaninejad S., Moghadam M., Mirkhani V., Mohammadpoor-Baltork I. (2012), MIL–101 metal–organic framework: A highly efficient heterogeneous catalyst for oxidative cleavage of alkenes with H_2O_2, *Catal. Commun.*, 17, pp. 18–22.

9. Férey G., Mellot-Draznieks C., Serre C., Millange F., Dutour J., Surblé S., Margiolaki I. (2005), A chromium terephthalate-based solid with unusually large pore volumes and surface area, *Science*, 309, pp. 2040–2042.

10. Khan N. A., Kang I. J., Seok H. Y., Jhung S. H. (2011), Facile synthesis of nano-sized metal-organic frameworks, chromium-benzene dicarboxylate, MIL–101, *Chem. Eng. J.*, 166, pp. 1152–1157.

11. Hirscher B. P. A. (2005), Hydrogen Physisorption in Metal–Organic Porous Crystals, *Advanced Materials*, 17(5), pp. 538–541.

12. Li Y., Yang R. T. (2007), Gas Adsorption and Storage in Metal−Organic Framework MOF–177, *Langmuir*, 23(26), pp. 12937–12944.